POLITECNICO DI TORINO
Repository ISTITUZIONALE

Optimization of Source/Relay Wireless Networks with Multiuser Nodes

Original
Optimization of Source/Relay Wireless Networks with Multiuser Nodes / Nordio, Alessandro; Chiasserini, Carla Fabiana; Tarable, Alberto. - In: IEEE TRANSACTIONS ON WIRELESS COMMUNICATIONS. - ISSN 1536-1276. - STAMPA. - 13:11(2014), pp. 6108-6117. [10.1109/TWC.2014.2345372]

Availability:
This version is available at: 11583/2557139 since:

Publisher:
IEEE - INST ELECTRICAL ELECTRONICS ENGINEERS INC

Published
DOI:10.1109/TWC.2014.2345372

Terms of use:

This article is made available under terms and conditions as specified in the corresponding bibliographic description in the repository

Publisher copyright

(Article begins on next page)

12 October 2024

Optimization of Source/Relay Wireless Networks with Multiuser Nodes

Alessandro Nordio, *Member, IEEE,* Carla-Fabiana Chiasserini, *Senior Member, IEEE,* and Alberto Tarable, *Member, IEEE*

***Abstract*—We compute the optimal communication rate achieved by the nodes of a wireless multihop network with arbitrary topology. The network nodes operate in half-duplex mode and generate information that has to be delivered to a gateway node, possibly through a decode-and-forward relaying strategy. Nodes may make use of multiuser processing, thus transmissions from multiple nodes toward the same receiver are allowed. Additionally, nodes may be energy-constrained, as in the case of battery-powered or energy-harvesting communication networks. In such scenario, we define the possible (and meaningful) network operational states. Then, by solving a linear optimization problem, we select the most efficient network states and for how long the network should work in each of them. More specifically, the resulting communication strategy maximizes the data rate achievable by the network while meeting the constraints that may exist on the node energy consumption. The results we present show how our approach can be effectively used for an optimal design and usage of wireless networks, as well as under which conditions multiuser processing and long-distance communication between nodes are most beneficial.**

I. Introduction

Wireless multihop networks are receiving increasing attention as they find application in environmental monitoring through sensors, dissemination of social content, and mesh communication backbone. In most of these contexts, one of the most critical aspects is to ensure high bit rates and low energy consumption.

In order to address such issues, several algorithms and protocols have been recently proposed in the literature. As an example, the works in [1]–[3] present energy-efficient communication schemes that specifically target sensor networks. Others adopt an information-theoretic approach to study traffic relaying in wireless networks. In particular, [4], [5] study networks where sources transfer their data by means of other nodes that act as relays only. The studies in [6], [7], instead, consider nodes that are both sources and relays, and that operate in full-duplex mode (i.e., nodes can transmit and receive at the same time). A similar network scenario is addressed in [8] but with few half-duplex nodes (i.e., nodes cannot transmit and receive at the same time), or in [9], [10] where however nodes do not interfere with each other as they transmit on orthogonal channels.

A. Nordio and A. Tarable are with the Institute of Electronics, Computer and Telecommunication Engineering of the National Research Council of Italy (IEIIT-CNR), Torino, Italy. e-mail: {alessandro.nordio, alberto.tarable}@ieiit.cnr.it

C.-F. Chiasserini is with Politecnico di Torino, Torino, Italy and is also a Research Associate with the Institute of Electronics, Computer and Telecommunication Engineering of the National Research Council of Italy (IEIIT-CNR), Torino, Italy. e-mail: chiasserini@polito.it

Similarly to some of the above studies, we adopt an information-theoretic perspective and investigate a wireless multihop with arbitrary topology whose nodes operate in half-duplex mode. Each node may generate traffic at different data rate to be delivered to a gateway node. If there is no direct link from the node to the gateway, the traffic generated by that node will have to reach the destination through a certain number of successive hops. In this case, the information produced at the source is relayed by other nodes to the gateway. For this reason, such multihop network is also referred to as source/relay wireless network. We will assume that, while acting as relays, nodes adopt the decode-and-forward (DF) strategy [4]. Furthermore, in order to achieve higher data rates, we allow multiuser detection (MUD) at the network nodes, although we do not go into details in the way it is practically realized. Finally, we are concerned with the node energy consumption and assume that it cannot exceed a maximum value, which is, possibly, different over the nodes. Such a constraint arises from green-communication considerations, and also from the fact that, in sensor networks for environmental monitoring [11], the nodes are either battery-powered or harvest energy from the environment. Based on what we have said before, it is clear that the network nodes consume power both for transmitting their own information and for relaying other nodes' traffic.

In the scenario under study, the choice of the communication and routing strategy to be adopted is crucial, as it determines which communication links should be activated and at which time instants, as well as the power level at which the nodes should transmit. We thus define the possible (but meaningful) network states, where a state corresponds to a set of active links, to the rate at which each link is used and to the corresponding transmitted power. Then, we formulate optimization problems so as to derive communication strategies that maximize the data rate achievable by the network and meet the constraints on the energy consumption experienced by the nodes. It turns out that the optimization can be formulated as a linear programming (LP) problem, whose solution tells us how long the network has to stay in any given state.

We highlight that our study significantly differs from previous work. In particular, in [12], a similar LP tool is described in order to optimize a source/relay network. However, the network considered in [12] has a linear topology and no multiuser processing is allowed, since only point-to-point links are considered. A linear network is considered also in [13], where each link between adjacent nodes is assumed to be error-free. In other papers [14], [15], the main goal is to

minimize the total energy consumption of the network, without considering that the nodes that are close to the gateway consume more power than the other nodes. Some other works aim at the maximization of the network lifetime [16], [17]. In particular, in [16], LP is applied to maximize the time before the first node in an ad-hoc network runs out of battery. This is achieved by optimizing the data rates at the network layer. Our goal instead is to maximize the data rate at the physical layer, by designing an optimal scheduling at the MAC layer that accounts for interference and power consumption. As for [17], it considers the transmission rates of the nodes to be fixed model parameters, while in our approach they are the result of the optimization. In [18], bounds and approximations for the achievable throughput are derived through optimal power control. However, the study in [18] is limited to a single-hop network and does not account for MUD. The study in [19] analyzes the achievable rate in a Gaussian multi-way relay channel, where all users have to share their data through a single relay. Again, the network topology is very different from the one we investigate, i.e., a multihop network where all nodes can act as sources and relays and data are collected at one gateway node.

For what concerns multiuser processing, its exploitation in the context of wireless network optimization appears in several papers in the literature. Among the most relevant to our work, [20] describes a multiantenna scheme for a multisource, single-relay, 2-hop network, where interference cancellation is used on the first hop and TDMA on the second hop. The study in [21] proposes a multiantenna, multisource, multirelay, 2-hop network where linear multiuser detectors are employed at the destination. In [22] the problem of beamforming optimization for a single-antenna, multisource, multirelay, 2-hop network is faced. A larger MIMO (multiantenna) mesh network is optimized in [23], but without interference among the links. Finally, we mention that a preliminary version of our work can be found in the conference paper [24].

The rest of the paper is organized as follows. Section II introduces the network scenario under study. The network states are defined in Section III; there, we also formulate the LP problem whose solution provides the strategy that maximizes the rate achievable by the network. In Section IV, the problem is particularized to two case studies: an additive white Gaussian noise (AWGN) channel model, and a system where the average power consumption of each node is limited to a maximum value. Section V shows some examples of how our analysis can be exploited for the study and design of wireless networks. Finally, Section VI draws our conclusions.

II. System model

We consider a wireless network composed of N stationary nodes and a gateway, which are arbitrarily deployed in a geographical region. Each node is labeled with an integer from[1] $[N+1]$, where node $N+1$ is the gateway. The set of integers $\{1,\dots,N\}$ is shortly denoted with $[N]$. Nodes communicate by sharing the same radio channel and are sources of independent, unicast traffic messages to be delivered to the gateway. We assume that the nodes are saturated, i.e., they always have traffic to transmit, and that each node n, $n \in [N]$, generates information with rate

$$W_n = \rho_n R\,. \tag{1}$$

The coefficients ρ_n are input parameters accounting for the different amount of information that each node is expected to generate in the unit time. Note that the aforementioned assumptions allow us to study the maximum fair rate allocation to all nodes, i.e., the average data rates that can be achieved by the nodes and that satisfy the desired proportion among the data generation rates. Clearly, considering that our objective is to compute the maximum achievable rate, from (1) it follows that the rate R should be maximized.

Another important feature of the communication nodes that our work takes into account is the capability to perform MUD. In particular, in our analysis we will assume that nodes can perform either MUD or single-user processing, and we will derive results under both scenarios. We remark that MUD is widely used in wireless networks and that when the number of simultaneous transmitters is small, as in our case, the receiver complexity can be significantly reduced [25].

Next, looking at the network topology, we observe that in practical applications a direct (i.e., one-hop) link between a node and the gateway can be established only if the signal-to-noise ratio (SNR) of such link is sufficiently high. If this condition does not hold, a node has to exploit multihop routes, i.e., to relay on other intermediate nodes to deliver its traffic to the gateway. The SNR of a radio link between two nodes depends on many parameters, such as the path loss, the transmit power, the antenna gains and the presence of obstacles or scatterers. Since nodes are stationary, we assume that radio channel conditions are static or change slowly with respect to the periodicity with which the link scheduling is updated. Furthermore, we assume that a scheme for neighbor discovery is implemented, as done by numerous technologies for ad-hoc and sensor networks. Through HELLO messages, such schemes also allow a node to detect changes in its neighborhood, i.e., in the set of its radio links, as well as in the link quality level.

Given the set of available radio links, the wireless network can be seen as a graph with $N+1$ vertices (the N nodes plus the gateway) connected by L edges representing the links, labeled with the integer numbers from $[L]$. Links are directed (or oriented): a link $\ell \in [L]$ has tail (or origin) in node $n = t(\ell)$ and head (or destination) in node $n' = h(\ell)$ if it is directed from node n to node n'. When labeling links, we sort them according to their head, i.e., first we label all links with $h(\ell) = 1$, if any, then all links with $h(\ell) = 2$, and so on. The orientation follows the information flow towards the gateway and is determined by using the geographical routing approach [26]. Thus, links are directed towards those nodes which are closer to the gateway than their origin. In the case where a node does not have any neighbor closer to the gateway than itself, the link points to those of its neighbors that can reach the gateway through other nodes. Note that this approach has several advantages: (i) it prevents having loops in the network topology graph, (ii) it

[1]The set of integers $\{1,\dots,Z\}$ is shortly denoted with $[Z]$.

allows each transmitter to have several potential receivers so as to balance the traffic load across multiple nodes, and (iii) it avoids detours which typically imply longer paths, higher traffic load and, hence, higher interference level. Note however that our analysis aims not at optimizing traffic routing, but at maximizing the achievable data rate at the physical rate by designing an optimal link scheduling. The information on the set of available radio links and possible receivers for each network node is known to the gateway, which, upon changes in the link set or in the link rates, computes a new link scheduling as detailed below and issues the communication strategy to all network nodes.

III. Network states and optimal communication strategies

In this section, we first introduce the concept of network states and explain how they are built in our model. Then, we formulate the LP problem that is the basis for the optimization of the network communication protocol. In Table I, we summarize the symbols used throughout the paper. We also adopt the following notation. Column vectors and matrices are denoted by bold lowercase and bold upper case letters, respectively. The transpose operator is denoted by $(\cdot)^{\mathsf{T}}$.

We define a link ℓ, directed from node $n = t(\ell)$ to node $n' = h(\ell)$, as *active* if node n is using that link to communicate to node n', i.e., if node n' is receiving information transmitted by node n. When a node is neither transmitting nor receiving, it is assumed to be in sleep state. At any given time instant, we group simultaneously active links in the subset $\mathcal{L}_\lambda \subseteq [L]$, with $\lambda \in [\Lambda]$, where Λ is the number of possible subsets of active links. An example clarifying the definition is provided below. We observe that such a number is potentially very large (i.e., $\Lambda \leq 2^L - 1$) and rapidly increasing with the number of links, L. However, it greatly reduces by taking into account the following constraints:

(i) nodes work in half-duplex mode, i.e., they cannot transmit and receive at the same time. Thus, a node cannot be simultaneously a transmitter for link ℓ and a receiver for link ℓ', when $\ell, \ell' \in \mathcal{L}_\lambda$;

(ii) each transmitting node has a single receiver, as we only consider unicast traffic transmissions. Indeed, enabling multiple receivers could improve the performance but it would also imply that multiple information streams coming from the same transmitter would flow over the network. At each hop, the number of streams would possibly increase as many times as the number of receivers at that hop. In certain cases, instead, some streams could merge into the same receiver. In this scenario, the problem would become mathematically intractable while the benefit in terms of performance is expected to be very low [27]. However, in our work we do allow a node to receive from several neighbors and perform multiuser processing [28].

The sets of active links satisfying the above constraints can be obtained through exhaustive search on the network graph, as shown in the example below.

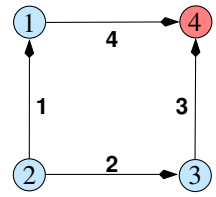

Fig. 1. A simple network with $N = 3$ nodes and $L = 4$ links. Node 4 is the gateway.

Example 1: Figure 1 shows a simple network with $N = 3$ nodes plus the gateway, and $L = 4$ links. By inspection, it turns out that there are $\Lambda = 7$ active link sets satisfying the constraints, namely:

$$\mathcal{L}_1 = \{1\} \quad \mathcal{L}_2 = \{2\} \quad \mathcal{L}_3 = \{3\} \quad \mathcal{L}_4 = \{4\}$$
$$\mathcal{L}_5 = \{1,3\} \quad \mathcal{L}_6 = \{2,4\} \quad \mathcal{L}_7 = \{3,4\}$$

Notice that in active link sets $\mathcal{L}_5$ and $\mathcal{L}_6$ two interfering links are simultaneously active. Moreover, in $\mathcal{L}_7$, node 4, which is the gateway, performs multiuser processing on the information that it receives through links 3 and 4, since $h(3) = h(4) = 4$.

Any communication strategy transferring information from the network nodes to the gateway can be built from a set of J network states $\sigma_1, \ldots, \sigma_J$, each active for a time fraction $\theta_1, \ldots, \theta_J$, respectively, where $\sum_{j=1}^{J} \theta_j = 1$. In our model, the j-th network state, $j \in [J]$, is completely specified by a set of active links, $\mathcal{L}_{\lambda(j)}$, $\lambda(j) \in [\Lambda]$, and by the vector of rates that are used to communicate on each link in that state, denoted by $\mathbf{r}_j = [r_j^1, \ldots, r_j^L$ where $r_j^\ell = 0$ if $\ell \notin \mathcal{L}_{\lambda(j)}$, i.e., the communication rate on the inactive links is zero. In our model some network states can be characterized by the same active link set, $\mathcal{L}_\lambda$. Therefore for every $\lambda \in [\Lambda]$, their corresponding rate vectors are listed in the set

$$\mathcal{R}_\lambda = \{\mathbf{r}_j : \lambda(j) = \lambda\} \tag{2}$$

of cardinality $|\mathcal{R}_\lambda| = K(\lambda)$. As it will be explained later, for those sets $\mathcal{L}_\lambda$ where no node simultaneously receives from more than one transmitter (i.e., where no multiuser processing is involved), we specify a single rate for each link $\ell \in \mathcal{L}_\lambda$, hence $K(\lambda) = 1$. Otherwise, for the active link sets where some nodes do perform MUD, more than one rate can be associated with a link, depending on the point of the corresponding multiuser capacity region at which the transmitters operate. In this case we have $K(\lambda) > 1$, so as to take into account all possible communication rates achieving the capacity over the multiuser channel.

In conclusion, we can denote the j-th network state by

$$\sigma_j = \left\{\mathcal{L}_{\lambda(j)}, \mathbf{r}_j\right\}, \;\; j \in [J] \tag{3}$$

where $\mathbf{r}_j \in \mathcal{R}_{\lambda(j)}$. The total number of states is then given by

$$J = \sum_{\lambda=1}^{\Lambda} K(\lambda) \tag{4}$$

The example below further clarifies these concepts.

TABLE I
SYMBOLS USED THROUGHOUT THE PAPER.

N, L	Number of nodes and links in the network
$W_n = \rho_n R$, $n \in [N]$	Rate of information generation at node n
$t(\ell) \in [N]$, $h(\ell) \in [N+1]$, $\ell \in [L]$,	Tail (or origin) and head (or destination) of link ℓ
J	Number of possible network states
θ_j, $j \in [J]$	Time fraction spent by the network in the j-th state
Λ	Number of possible active link sets
$\mathcal{L}_\lambda$, $\lambda \in [\Lambda]$	The λ-th active link set
$\mathcal{L}_{\lambda(j)}$, $j \in [J]$, $\lambda(j) \in [\Lambda]$	The active link set in the j-th network state
$K(\lambda)$, $\lambda \in [\Lambda]$	Number of network states with active link set $\mathcal{L}_\lambda$
r_j^ℓ, $j \in [J]$, $\ell \in [L]$	Communication rate on link ℓ in the j-th network state
$\mathbf{r}_j = [r_j^1, \ldots, r_j^L]$, $j \in [J]$	The rate vector for all links in the j-th network state
$\mathcal{R}_\lambda = \{\mathbf{r}_j : \lambda(j) = \lambda\}$, $\lambda \in [\Lambda]$	The set of possible rate vectors associated with active link set $\mathcal{L}_\lambda$
$\mathcal{L}_\lambda(n) \subseteq \mathcal{L}_\lambda$, $\lambda \in [\Lambda]$, $n \in [N+1]$	Multiuser subgroup with receiving node n in active link set $\mathcal{L}_\lambda$
$k_\lambda(n)$, $\lambda \in [\Lambda]$, $n \in [N+1]$	Size of $\mathcal{L}_\lambda(n)$
$\mathcal{I}_\lambda(n) \subset [N]$, $\lambda \in [\Lambda]$, $n \in [N+1]$	Tails of links outside $\mathcal{L}_\lambda(n)$ in active link set $\mathcal{L}_\lambda$
$\mathbf{v}_\lambda^\kappa(n)$, $\kappa \in [k_\lambda(n)!]$, $\lambda \in [\Lambda]$, $n \in [N+1]$	The κ-th vertex of the dominant face in the multiuser capacity region for $\mathcal{L}_\lambda(n)$
$C_\lambda^{\mathcal{S}}(n)$, $\mathcal{S} \subseteq \mathcal{L}_\lambda(n)$, $\lambda \in [\Lambda]$, $n \in [N+1]$	Capacity limit on the sum-rate for a subset $\mathcal{S}$ of the links in $\mathcal{L}_\lambda(n)$
$\mathcal{R}_\lambda(n) = \{\mathbf{v}_\lambda^\kappa(n),\ \kappa \in [k_\lambda(n)!]\}$, $\lambda \in [\Lambda]$, $n \in [N+1]$	Set of vertices of the dominant face in the multiuser capacity region for $\mathcal{L}_\lambda(n)$
$\mathbf{R}$	$L \times J$ matrix whose j-th column is given by $\mathbf{r}_j$
$\mathbf{H}$	$L \times N$ matrix such that $(\mathbf{H})_{\ell n} = 1$ if node $n = h(\ell)$ and 0 otherwise
$\mathbf{T}$	$L \times N$ matrix such that $(\mathbf{T})_{\ell n} = 1$ if $n = t(\ell)$ and 0 otherwise
P_e	Reference power level
$\gamma(n, n')$, $n, n' \in [N+1]$	Received SNR at node n' for the signal transmitted by node n with power P_e
$\alpha_\lambda(n)$, $\lambda \in [\Lambda]$, $n \in [N]$	Normalized irradiated power by node n in the active link set $\mathcal{L}_\lambda$
$I_\lambda(n)$, $\lambda \in [\Lambda]$, $n \in [N+1]$	Amount of interference received by node n in the active link set $\mathcal{L}_\lambda$
$\widetilde{\mathbf{H}}$	$N \times J$ matrix s. t. $(\widetilde{\mathbf{H}})_{nj} = 1$ if node n is receiving in state j and 0 o.w.
$\widetilde{\mathbf{T}}$	$N \times J$ matrix s. t. $(\widetilde{\mathbf{T}})_{nj} = 1$ if node n is transmitting in state j and 0 o.w.
$\boldsymbol{\pi} = [\pi(1), \ldots, \pi(N)]$	Normalized average power consumption for all nodes

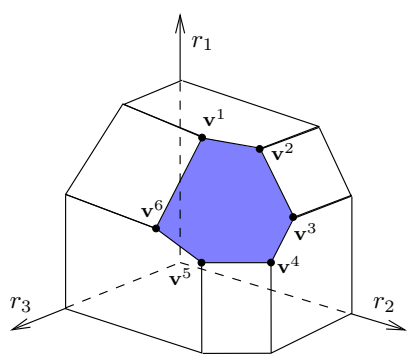

Fig. 3. Capacity region of a multiuser channel defined by $k = 3$ wireless links. The dominant face is highlighted in blue. The $k! = 6$ vertices have coordinates $\mathbf{v}^\kappa$, $\kappa \in [6]$. Every point of the dominant face can be expressed through a convex combination of rates associated with the vertices $\mathbf{v}^\kappa$.

Example 2: The network of Figure 1, whose active link sets are listed in Example 1, can be in one out of $J = 8$ possible states, since $K(\lambda) = 1,\ \ \lambda \in [6]$ and $K(7) = 2$. Indeed, the active link set $\mathcal{L}_7$ is the only one where MUD is performed (at the gateway). If we number the states so that $\mathcal{L}_{\lambda(j)} = \mathcal{L}_j$, for $j \in [6]$ and $\mathcal{L}_{\lambda(j)} = \mathcal{L}_7$ for $j = 7, 8$, we can write the rate vectors for the last two states as:

$$\mathbf{r}_7 = (0, 0, r_7^3, r_7^4), \quad \mathbf{r}_8 = (0, 0, r_8^3, r_8^4)$$

The way rate vectors are actually computed for a general network is explained later in the paper.

Next, for each set of active links $\mathcal{L}_\lambda$ we show how to compute the rate vectors in the set $\mathcal{R}_\lambda$ and its cardinality $K(\lambda)$. To this end, we first observe that $\mathcal{L}_\lambda$ can be partitioned into disjoint subsets $\mathcal{L}_\lambda(n)$, $n \in [N+1]$, where

$$\mathcal{L}_\lambda(n) = \{\ell \in \mathcal{L}_\lambda | h(\ell) = n\}$$

is the set of active links having node n as a common receiver. From the above definitions, it follows that node $n \in [N+1]$

- simultaneously receives useful signals from $k_\lambda(n) = |\mathcal{L}_\lambda(n)|$ neighbors,
- receives interference from the set of interfering transmitters $\mathcal{I}_\lambda(n) = \{t(\ell) | \ell \in \mathcal{L}_\lambda \setminus \mathcal{L}_\lambda(n)\}$.

In order to clarify these concepts and definitions, we provide the following example.

Example 3: Figure 2 (left) shows a network with $N+1 = 6$ nodes (including the gateway) and $L = 10$ links. We consider a specific network state, which is depicted in Figure 2 (right) where active links are denoted by solid lines, while inactive links are indicated by dashed lines. To ease the notation, we drop the subscript λ. The set of active links, $\mathcal{L} = \{2, 3, 9\}$, can be written as

$$\mathcal{L} = \mathcal{L}(3) \cup \mathcal{L}(6)$$

where $\mathcal{L}(3) = \{2, 3\}$ and $\mathcal{L}(6) = \{9\}$. That is, node 3 is receiving from $k(3) = |\mathcal{L}(3)| = 2$ nodes and node 6 (the gateway) is receiving from $k(6) = |\mathcal{L}(6)| = 1$ node. All other nodes are not receiving (i.e., $\mathcal{L}(n) = \emptyset$, for $n = 1, 2, 4, 5$). Node 3 receives interference from the nodes in the set $\mathcal{I}(3) = \{4\}$, while node 6 receives interference from the nodes in $\mathcal{I}(6) = \{1, 2\}$.

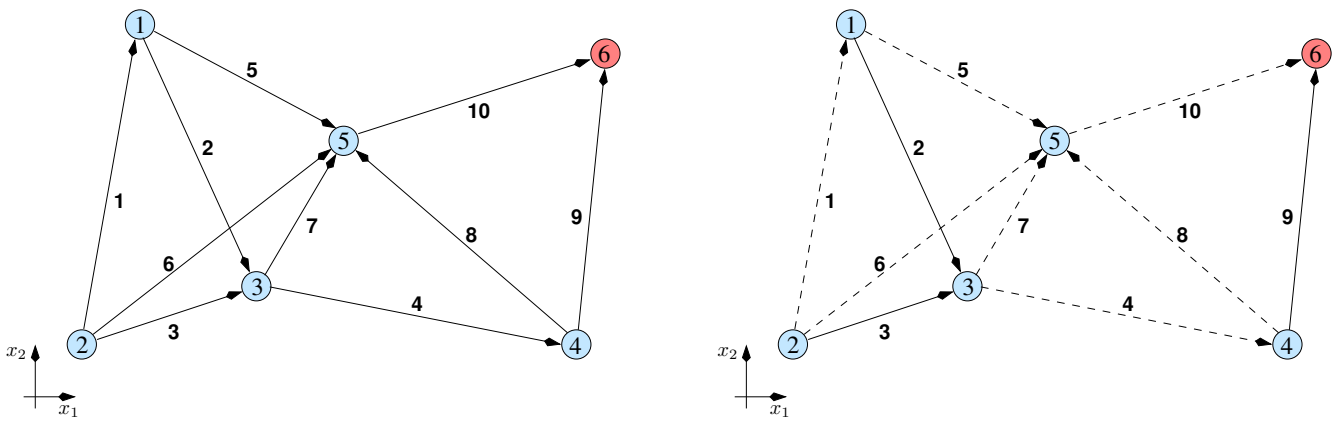

Fig. 2. Example of a network with $N = 5$ nodes and $L = 10$ links. Node 6 represents the gateway. The image on the left shows the whole network graph while the right image shows an example of a network state where active and inactive links are marked by solid and dashed lines, respectively.

When a node receives simultaneously from $k \geq 1$ wireless active links and performs MUD, the achievable rates associated to such links are contained in the corresponding multiuser capacity region [4]. More specifically, the highest achievable sum-rates are represented by the Pareto-optimal points in the dominant face of the capacity region, which is a convex polytope of dimension $k-1$ and is obtained as the convex hull of $k!$ vertices. Therefore, any point on the dominant face of the capacity region can be expressed through a convex combination of the rates associated with the face vertices. The rates achieved by the k links at the κ-th vertex ($\kappa \in [k!]$) of the dominant face are denoted by

$$\mathbf{v}^{\kappa} = (v^{\kappa,1}, \ldots, v^{\kappa,k}) \,. \tag{5}$$

and can be expressed in terms of the limits $C^{\mathcal{S}}$, defining the capacity region [4], where $\mathcal{S}$ is a non-empty subset of the active link set. The limit $C^{\mathcal{S}}$ represents the maximum achievable sum-rate for the links in $\mathcal{S}$.

Figure 3 presents an example of a multiuser capacity region with active links $\{1,2,3\}$ and $k = 3$. The dominant face is highlighted in blue and the vertices are denoted by $\mathbf{v}^{\kappa}$, $\kappa \in [6]$. Each vertex is associated to a permutation of $\{1,2,3\}$. In particular vertex $\mathbf{v}^1$ is associated to the permutation (132) in the following sense: we first consider link 1 and saturate its rate to the largest possible value, which is $v^{1,1} = C^{\{1\}}$; then we consider link 3 and again saturate its rate to the largest possible value, compatibly with the value of $v^{1,1}$, which is $v^{1,3} = C^{\{1,3\}} - C^{\{1\}}$; and finally we assign link 2 the rate $v^{1,2} = C^{\{1,2,3\}} - C^{\{1,3\}}$, which is the largest possible rate compatible with the previous choices for the other two links. Analogously, vertex $\mathbf{v}^2$ is associated to the permutation (123), and so on.

Going back to our system model, when node n receives from the links in the active link set $\mathcal{L}_\lambda(n)$ the rate vectors $\mathbf{v}^{\kappa}_{\lambda}(n)$, $\kappa \in [k_\lambda(n)!]$, can be expressed in terms of the limits $C^{\mathcal{S}}$ where $\mathcal{S} \subseteq \mathcal{L}_\lambda(n)$. We then define the set of rate vectors achieved at the $k_\lambda(n)!$ vertices of the dominant face of the corresponding multiuser capacity region as

$$\mathcal{R}_\lambda(n) = \{\mathbf{v}^{\kappa}_{\lambda}(n), \;\; \kappa \in [k_\lambda(n)!]\} \,.$$

Since there are $k_\lambda(n)!$ vertices associated to the capacity region of each receiving node n ($n \in [N+1]$), then for every $\mathcal{L}_\lambda$ the total number of rate vectors is

$$K(\lambda) = \prod_{n=1}^{N+1} k_\lambda(n)! \,. \tag{6}$$

The rate vector set $\mathcal{R}_\lambda$ appearing in (2) is then given by the Cartesian product

$$\mathcal{R}_\lambda = \mathcal{R}_\lambda(1) \times \cdots \times \mathcal{R}_\lambda(N+1) \,.$$

Again, in order to clarify the concepts and notations that we provide the example below, referring to the network in Figure 2.

Example 4: For the network of Figure 2 (left), the number of rate vectors associated with the active link set shown in Figure 2 (right) is given by

$$K(\lambda) = \prod_{n=1}^{N+1} k_\lambda(n)! = k_\lambda(3)! k_\lambda(6)! = 2 \,.$$

Thus, this choice of active links involves $K(\lambda) = 2$ network states. Let us drop the subscript λ for ease of notation. The rate vectors that can be achieved in the multiuser subgroup with receiving node 3 (for which $k(3) = 2$) are given by $\mathbf{v}^1(3) = (v^{1,1}(3), v^{1,2}(3))$ and $\mathbf{v}^2(3) = (v^{2,1}(3), v^{2,2}(3))$ where $v^{1,1}(3) = C^{\{1\}}(3)$, $v^{1,2}(3) = C^{\{1,2\}}(3) - C^{\{1\}}(3)$, $v^{2,1}(3) = C^{\{2\}}(3)$, and $v^{2,2}(3) = C^{\{1,2\}}(3) - C^{\{2\}}(3)$ with obvious notation. Thus, $\mathcal{R}(3) = \{\mathbf{v}^1(3), \mathbf{v}^2(3)\}$. Regarding receiving node 6, we have trivially $\mathbf{v}^1(6) = (v^{1,1}(6))$, with $v^{1,1}(6) = C^{\{1\}}(6)$ and $\mathcal{R}(6) = \{\mathbf{v}^1(6)\}$. Therefore, the sets of rate vectors $\mathcal{R}$ is given by the Cartesian product $\mathcal{R} = \mathcal{R}(1) \times \cdots \times \mathcal{R}(6) = \{\mathbf{r}_1, \mathbf{r}_2\}$, where

$$\mathbf{r}_1 = (0, v^{1,1}(3), v^{1,2}(3), 0, 0, 0, 0, 0, 0, v^{1,1}(6))$$

$$\mathbf{r}_2 = (0, v^{2,1}(3), v^{2,2}(3), 0, 0, 0, 0, 0, 0, v^{1,1}(6))$$

We hasten to observe that, with this choice of the network states, *every* point in the dominant face of the multiuser

capacity region for any multiuser subgroup can be reached. Indeed, since every such point is the convex combination of the vertices $\mathbf{v}^\kappa$, the state time fractions θ_j, $j \in [J]$, identify for any multiuser subgroup a unique point which is not necessarily a vertex and lies anywhere in the dominant face. An explicit example will be given in Section V.

In the following proposition, we give upper and lower bounds to the number of states J for a given network size.

Proposition 3.1: Consider a network with $N+1$ nodes (including the gateway). Then, the number of states J satisfies

$$F_{N+2} - 1 \leq J \leq (N+1)! - 1 \tag{7}$$

where F_n is the n-th Fibonacci number.

Proof: It can be easily seen that the number of states increases with the number of available links L. The lower bound is achieved by the connected network with the minimum value of L, i.e., $L = N$. Among all networks with N links, the one with the minimum number of states corresponds to a linear topology, where MUD is not possible. Then, from [12], we obtain the lower bound in (7).

By the same reasoning, the upper bound is obtained by considering a fully connected network, where $L = \frac{N(N-1)}{2}$. In such a case, let us number the nodes starting from the one that is farthest away from the gateway and proceeding toward the gateway. Thus, node n can transmit to node n' if and only if $n < n'$. We can map a given state of the network into a permutation of the set $[N+1]$ as follows:

- we sort the set of nodes that are either in receiving or in sleep mode in increasing order, and
- we insert immediately after a given receiving node the set of nodes that are transmitting to it; for MUD, the order of the transmitting nodes identifies a cornerpoint of the capacity region.

For example, if $N+1 = 5$, the permutation (43215) identifies the state where node 4 receives from nodes 1, 2 and 3, with the rates corresponding to the cornerpoint $\mathbf{v}_5$ in Fig. 3, while node 5 (the gateway) is in sleep mode. It is easy to see that each permutation identifies a unique state and vice versa, with the only exception of the permutation $(12\cdots N)$, which would identify a state where all nodes are in sleep mode. Thus, the total number of states for the fully connected network is equal to the total number of permutations of $[N+1]$ minus one, giving the upper bound of (7). ■

The bounds on J of (7) impose some constraints on the values of N for which our method, described below, can be applied. However, it is worth noting that the upper bound is rather pessimistic and that a sparse network has a number of states considerably smaller than $(N+1)! - 1$. For example, the network in Fig. 2 (left) has only $J = 133$ possible states, instead of 719, which is the upper bound for $N+1 = 6$.

Furthermore, simple yet effective techniques to reduce the number of states can be adopted. For example, we can divide the network area into subregions, and the network into subnetworks, one for each subregion. For each subnetwork, we can identify a number of "intermediate gateways" that can transfer traffic from the subregion to another, which is closer to the final gateway. Thus, it is possible to compute the states for each subnetwork with low complexity and then combine them properly, so that all network states can be easily obtained. In light of this, the search of the possible network states implies a limited delay.

A. Optimal communication strategies

Next, we derive the optimal communication strategies that maximize rate R. Recall that the generic node n generates information at rate W_n. It also receives information from its predecessors in the network graph (i.e., from those nodes which are origins of the links directed to n) and forwards it to its successors (i.e., to those nodes that are the destinations of the links originated in n). Relays adopt a DF [4] relaying strategy so that the received signals are decoded and then re-encoded before being forwarded towards the gateway.

The information flowing through node n has to obey to the basic flow equation:

$$W_n + \sum_{\ell | h(\ell)=n} \sum_{j=1}^{J} r_j^\ell \theta_j - \sum_{\ell | t(\ell)=n} \sum_{j=1}^{J} r_j^\ell \theta_j = 0 \tag{8}$$

where the second and third terms represent the information flow, respectively, received and transmitted by node n. Using (1), we can rewrite (8) in a more compact form as

$$\boldsymbol{\rho} R + (\mathbf{H} - \mathbf{T})^\mathsf{T} \mathbf{R} \boldsymbol{\theta} = \mathbf{0}$$

where $\boldsymbol{\rho} = [\rho_1, \ldots, \rho_n]^\mathsf{T}$, $\mathbf{R}$ is the $L \times J$ matrix whose j-th column is given by $\mathbf{r}_j$, and $\mathbf{H}$ and $\mathbf{T}$ are $L \times N$ Boolean matrices such that $(\mathbf{H})_{\ell n} = 1$ if node $n = h(\ell)$ and 0 otherwise, and $(\mathbf{T})_{\ell n} = 1$ if $n = t(\ell)$ and 0 otherwise.

Given the network graph, the vector $\boldsymbol{\rho}$ and the rate matrix $\mathbf{R}$, the rate R achieved by any communication strategy depends on the choice of the time fractions $\boldsymbol{\theta}$. The maximum achievable rate, R^*, can be obtained by solving the following LP problem

$$\begin{aligned} R^* \quad &= \quad \max_{\boldsymbol{\theta}} R \\ &\text{s.t.} \quad \boldsymbol{\rho} R + (\mathbf{H} - \mathbf{T})^\mathsf{T} \mathbf{R} \boldsymbol{\theta} = \mathbf{0} \\ &\qquad\quad \mathbf{1}^\mathsf{T} \boldsymbol{\theta} = 1, \quad \boldsymbol{\theta} \geq \mathbf{0}\,. \end{aligned} \tag{9}$$

The vector of time fraction $\boldsymbol{\theta}^*$ maximizing (9) defines the communications strategy providing the highest possible data rate under the assumptions made above. We remark that, since the network nodes are assumed to be saturated, the operational states whose associated time fraction is greater than zero, can be activated in any order. From LP theory, we know that there will be at most N nonzero components in the optimal time fraction vector $\boldsymbol{\theta}^*$, so that the implementation is not dramatically complex. Also, we stress that non-integer LP problems can be solved in polynomial time and, in particular, our formulation is suitable to be solved in real time [29].

IV. Two case studies: AWGN and power constraints

In this section, we particularize the previous problem to two very important case studies. In Section IV-A, we consider the case of the additive white Gaussian noise (AWGN) channel model. In Section IV-B, we define a modified version of the

problem in (9), which takes into account constraints on the power consumption of each node; such constraints are relevant in many practical systems.

A. Optimal communication strategy for AWGN

In this section, we specify the problem in (9) for the particularly important case of transmission on the AWGN channel. More precisely, we define here the entries of the rate matrix $\mathbf{R}$ in (9).

We consider that the communication channel shared by the nodes has bandwidth W and is affected by AWGN with power spectral density level N_0 at all receivers. In the following, we define as $\gamma(n, n')$ the signal-to-noise ratio (SNR) at node n' when it receives a signal transmitted by node n at a reference power level P_e. Such definition has the only purpose to simplify the notation used throughout the paper; for concreteness, we set P_e equal to the node power consumption in receiving state, which is assumed to be equal for all nodes. In general, the value of the SNR depends on the characteristics of the propagation environment and may vary over time. In this work, however, we focus on static or slowly varying communication channels where the values of the SNRs, $\gamma(n, n')$, remain constant or do not significantly change for a sufficiently large amount of time.

Let us consider the multiuser subgroup $\mathcal{L}_\lambda(n)$. On the AWGN channel, the capacity limit for the generic subset $\mathcal{S} \subseteq \mathcal{L}_\lambda(n)$ is given by:

$$C_\lambda^{\mathcal{S}}(n) = \log_2 \left(\frac{\sum_{\ell \in \mathcal{S}} \alpha_\lambda(t(\ell))\gamma(t(\ell), n)}{1 + I_\lambda(n)} \right). \qquad (10)$$

where the interference received by node n is

$$I_\lambda(n) = \sum_{i \in \mathcal{I}_\lambda(n)} \alpha_\lambda(i)\gamma(i, n)\,.$$

$P_\lambda^{\text{tx}}(i)$ is the power irradiated by node i when the active link set is $\mathcal{L}_\lambda$ and

$$\alpha_\lambda(i) = P_\lambda^{\text{tx}}(i)/P_e\,. \qquad (11)$$

We now exploit the model introduced above to compute the maximum achievable rate R, in the case where the node average power consumption must be bounded by some target values, and we provide a formulation accounting for such constraints.

B. Optimal communication strategy under power constraints

The instantaneous power consumption of the generic node n, $n \in [N]$, depends on its state. As already mentioned, when the node is receiving, its consumption is equal to P_e, which is independent of the node index n. We model the power consumption of a transmitting node by $P_e + \alpha_\lambda(n)P_e = P_e(1 + \alpha_\lambda(n))$, where $P_\lambda^{\text{tx}}(n) = \alpha_\lambda(n)P_e$ is the power irradiated by node n when the set of active links is $\mathcal{L}_\lambda$. Moreover, we assume that the power irradiated by a node is limited, i.e., $P_\lambda^{\text{tx}}(n) \leq P_{\max}^{\text{tx}}$. Finally, when a node is in sleep state, its power consumption is assumed to be negligible. For simplicity, in the following all powers are normalized to the reference value P_e. In conclusion, the average normalized power required by node n is given by

$$\pi(n) = \sum_{j=1}^{J} \left(\tilde{t}_{n,j}(1 + \alpha_{\lambda(j)}(n))\theta_j + \tilde{h}_{n,j}\theta_j \right)\,, \qquad (12)$$

where $\tilde{t}_{n,j} = 1$ if node n is transmitting during state j, 0 otherwise. Similarly, $\tilde{h}_{n,j} = 1$ if node n is receiving during state j, 0 otherwise.

More compactly, the vector of average power consumption's $\boldsymbol{\pi} = [\pi(1), \ldots, \pi(N)]^\mathsf{T}$ can be written as

$$\boldsymbol{\pi} = (\widetilde{\mathbf{T}} + \mathbf{A})\boldsymbol{\theta} + \widetilde{\mathbf{H}}\boldsymbol{\theta} \qquad (13)$$

where the $N \times J$ matrix $\mathbf{A}$ is such that $(\mathbf{A})_{n,j} = \alpha_{\lambda(j)}(n)$ (clearly $(\mathbf{A})_{n,j} = 0$ if node n is receiving or in sleep state, in network state j). Also, we defined the $N \times J$ matrices $\widetilde{\mathbf{T}}$ and $\widetilde{\mathbf{H}}$ as $(\widetilde{\mathbf{T}})_{n,j} = \tilde{t}_{n,j}$ and $(\widetilde{\mathbf{H}})_{n,j} = \tilde{h}_{n,j}$.

Often in wireless networks it is required that the average node power consumption does not exceed a given target value. That is, the following inequalities must hold:

$$\boldsymbol{\pi} \leq \boldsymbol{\pi}^{\max} \qquad (14)$$

where $\boldsymbol{\pi}^{\max} = [\pi^{\max}(1), \ldots, \pi^{\max}(N)]^\mathsf{T}$ is the vector of constraints on the nodes average power consumption. Then, the problem in (9) has to be modified to take into account such constraints. Using (14) and (13), we rewrite (9) as

$$\begin{aligned} R^* \quad = \quad & \max_{\boldsymbol{\theta}} R \\ \text{s.t.} \quad & \boldsymbol{\rho} R + (\mathbf{H} - \mathbf{T})^\mathsf{T}\mathbf{R}\boldsymbol{\theta} = \mathbf{0} \\ & (\widetilde{\mathbf{T}} + \mathbf{A})\boldsymbol{\theta} + \widetilde{\mathbf{H}}\boldsymbol{\theta} \leq \boldsymbol{\pi}^{\max} \\ & \mathbf{1}^\mathsf{T}\boldsymbol{\theta} = 1, \quad \boldsymbol{\theta} \geq \mathbf{0}\,. \end{aligned} \qquad (15)$$

From LP theory, we know that there will be at most $2N$ nonzero components in $\boldsymbol{\theta}^*$ when accounting for power constraints, and that the number of excess nonzero components with respect to the N of the LP problem in (9) will be equal to the number of power constraints met with the equal sign.

V. Model exploitation

The strategy achieving the optimal rate R^* depends on many parameters, such as the network topology, the network load, the channel characteristics, the transmit powers, and the constraints that are imposed on the node average power consumption. Here we present an example of how our analysis can be applied to the study of a wireless network.

We focus on the network depicted in Figure 2 (left) with $N = 5$ nodes and a gateway (node 6). The nodes are deployed in a square region of side 100 m and their position is given by $\mathbf{x}_1$ =(20 m, 80 m), $\mathbf{x}_2$ =(10 m, 25 m), $\mathbf{x}_3$ =(40 m, 35 m), $\mathbf{x}_4$ =(95 m, 25 m), $\mathbf{x}_5$ =(55 m, 60 m). The gateway is at position $\mathbf{x}_6$ =(100 m, 75 m). Nodes use a bandwidth of $W =$ 1 MHz at 2.4 GHz, corresponding to a wavelength $\lambda = 1/8$ m. Unless otherwise specified, the channel is assumed to be static with propagation exponent $a = 3$.

Nodes are equipped with omnidirectional antennas and the noise power spectral density at each receiver is set to $N_0 = -174$ dBm/Hz. The power consumed by the nodes in receive

mode (i.e., the reference power) is set to $P_e = 1$ mW, while the power irradiated by the antennas is limited by $P_{\max}^{\text{tx}} = 1$ mW. Also, we assume that the nodes harvest energy from the environment and gather an average normalized power $\boldsymbol{\pi}^{\max} = [1.5, 1.5, 1.5, 1.5, 1.5]$. It follows that the node average power consumption cannot exceed 1.5.

Although in practice the propagation conditions are different for every node, in this example we make the simplifying assumption that a direct communication link between two nodes exists only if their distance is shorter than the radio range $d_r = 60$ m. This is a typical value for sensor networks; any other value could be considered as well. Under the above condition, the network in Figure 2 (left) has $L = 10$ links whose orientation has been chosen following the geographical routing approach described in Section II. We observe that nodes 3, 5, and 6 are the heads of more than one link, thus they can perform MUD.

An exhaustive search over the network graph allows to find $J = 133$ network states, among which two have been described in detail in the example given in Section III. We solve the linear problem in (9) (i.e., without taking into account the constraints on energy consumption) in the case where all nodes generate the same amount of information to be delivered to the gateway, i.e., $\rho_n = 1, n \in [N]$. We also assume that the power irradiated by transmitting nodes is set to $P_{\max}^{\text{tx}}$ for all states. We therefore obtain the rate $R^* = 0.333$ Mb/s that can be achieved by a communication strategy defined by the time fractions $\boldsymbol{\theta}^*$. In our case, we obtain the 5 active network states, which are reported in Table II. For each state index j, the table shows the corresponding time fraction θ_j^*, the set of active links $\mathcal{L}_{\lambda(j)}$, and the nonzero elements of the vector $\mathbf{r}_j$.

TABLE II
TIME FRACTIONS, ACTIVE LINKS AND RATES FOR THE NETWORK IN FIGURE 2.

j	θ_j^*	$\mathcal{L}_{\lambda(j)}$	$\{r_j^\ell, \ell \in \mathcal{L}_{\lambda(j)}\}$ [b/s/Hz]
8	0.100	$\{3, 9, 10\}$	$(0.706, 0.632, 1.530)$
12	0.533	$\{9, 10\}$	$(0.667, 1.730)$
38	0.138	$\{4, 10\}$	$(0.618, 1.260)$
111	0.019	$\{5, 6, 7\}$	$(2.255, 0.355, 1.397)$
112	0.210	$\{5, 6, 7\}$	$(1.388, 1.223, 1.397)$

The active links of the network states listed in Table II are also represented in Figure 4. We first observe that in states $j = 8$ and $j = 12$ the gateway receives useful signals from nodes 4 and 5 through links 1 and 2, respectively. Thus, it implements MUD. Node 5 also implements MUD in states $j = 111$ and $j = 112$ since it receives signals simultaneously from nodes 1,2, and 3. In particular, the rate vectors $\mathbf{r}_j$ in states $j = 111$ and $j = 112$ represent two of the vertices of a 3-user multiuser capacity region such as that depicted in Figure 3. Notice that the combination of these two vertices represents the optimal non-vertex point of the dominant face in the corresponding multiuser capacity region, since

$$\theta_{111}^* \mathbf{r}_{111} + \theta_{112}^* \mathbf{r}_{112} = (\theta_{111}^* + \theta_{112}^*) \left[\frac{\theta_{111}^*}{\theta_{111}^* + \theta_{112}^*} \mathbf{r}_{111} + \frac{\theta_{112}^*}{\theta_{111}^* + \theta_{112}^*} \mathbf{r}_{112} \right]$$

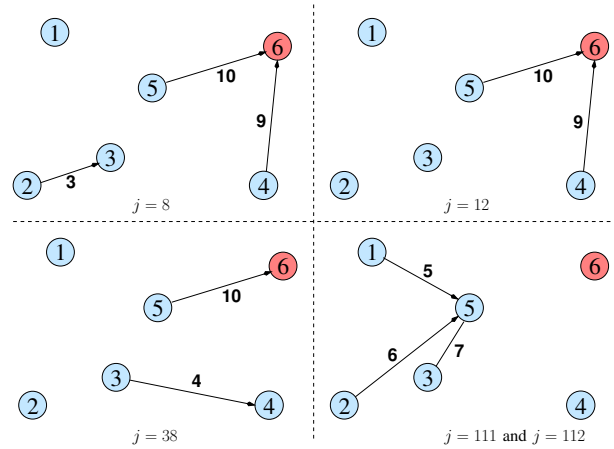

Fig. 4. Active links corresponding to the network states shown in Table II.

where the convex combination between brackets is the non-vertex point. As a practical consequence, the strategy can be implemented with only four network states, by directly implementing with probability $\theta_{111}^* + \theta_{112}^* = 0.229$ the optimal point, whose rate vector has nonzero components $(1.46, 1.151, 1.397)$ on $\mathcal{L}_{\lambda(111)}$. Interference between links that are simultaneously active appears in states $j = 8$ and $j = 38$, while it is absent in the others. The communication strategy described above requires the nodes to consume an average normalized power $\boldsymbol{\pi} = [0.457, 0.658, 0.833, 1.405, 1.771]$, which is obtained by computing (13).

We highlight that our proposed communication scheme can provide significant gains in terms of SNR with respect to simpler schemes that avoid the activation of interfering links. The benefit of allowing interfering links is outlined in Table III where we compare the rates (in Mb/s) achieved by the proposed scheme and by the interference-free communication scheme in [30]. The results refer to the same scenario as above and show the performance as $P_{\text{tx}}^{\max}$ varies.

We observe that when the transmit power is low, the interference does not reduce significantly the SINR and, thus, a gain (up to 30%) can be obtained by activating more links simultaneously. This gain decreases as the transmit power increases, since interference also increases. When the transmit power is high, the interference nullifies the gain provided by parallelism, thus the optimization problem in (9) does not select states with simultaneously active links. In such a situation, our strategy is equivalent to the interference-free communication scheme. Next, we look at the results

TABLE III
OUR STRATEGY VS. THE INTERFERENCE-FREE SCHEME FOR THE NETWORK IN FIGURE 2. RATES ARE EXPRESSED IN MB/S.

$P_{\text{tx}}^{\max}$ [mW]	0.1	0.2	0.5	1	2	5	10
Interf.	0.057	0.101	0.190	0.268	0.352	0.481	0.588
Interf.-free	0.044	0.079	0.154	0.233	0.326	0.468	0.588
Gain	30%	28%	23%	15%	8%	3%	0%

obtained above and observe that node 5 requires an average normalized power above the threshold of 1.5. If we constrain the node average normalized power to be limited by $\boldsymbol{\pi}^{\max} = [1.5, 1.5, 1.5, 1.5, 1.5]$, the solution of (15) provides a

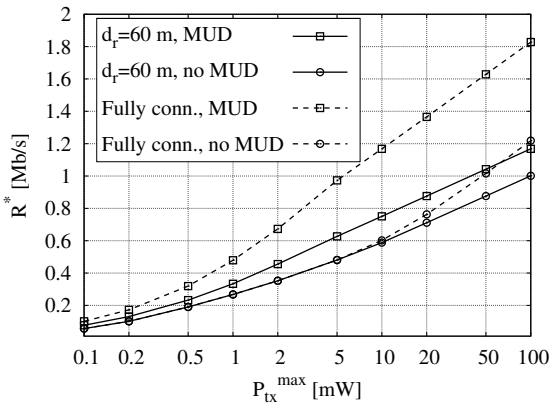

Fig. 5. Achieved rates for the network topology in Figure 2 (left) versus the maximum transmit power, $P_{\rm tx}^{\max}$, with and without MUD. Radio range: $d_r = 60$ and $d_r = 120\,$m (fully connected), and $a = 3$.

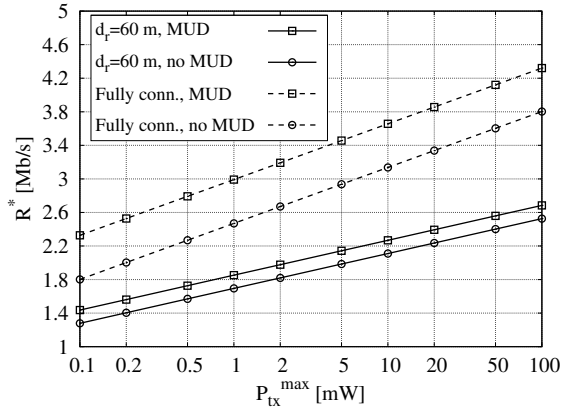

Fig. 6. Achieved rates for the network topology in Figure 2 (left) versus the maximum transmit power, $P_{\rm tx}^{\max}$, for the case with and without MUD, radio range $d_r = 60$ and $d_r = 120\,$m (fully connected), and $a = 2$.

rate $R^* = 0.316\,$Mb/s, which is lower than before. Indeed the new solution implies a different strategy with six (instead of five) active states, which are listed in Table IV. However, the

TABLE IV
TIME FRACTIONS, ACTIVE LINKS AND RATES FOR THE NETWORK IN FIGURE 2 UNDER THE CONSTRAINTS ON POWER CONSUMPTION

j	θ_j^*	$\mathcal{L}_{\lambda(j)}$	$\{r_j^\ell, \ell \in \mathcal{L}_{\lambda(j)}\}$ [b/s/Hz]
8	0.078	$\{3, 9, 10\}$	$(0.706, 0.632, 1.530)$
12	0.573	$\{9, 10\}$	$(0.667, 1.730)$
34	0.029	$\{3, 9\}$	$(2.083, 1.372)$
110	0.122	$\{4\}$	(1.272)
111	0.048	$\{5, 6, 7\}$	$(2.255, 0.355, 1.397)$
112	0.150	$\{5, 6, 7\}$	$(1.388, 1.223, 1.397)$

average normalized power consumption at the nodes becomes $\boldsymbol{\pi} = [0.396, 0.610, 0.747, 1.482, 1.500]$. We observe that the slight reduction in the achieved rate, with respect to the case without energy constraints, is traded off with a reduction in the power consumption of nodes 1,2,3, and 5.

In general by imposing constraints on the nodes average power consumption, lower rates are achieved and the optimal strategy shows a larger number of states with respect to the unconstrained case. In the extreme case where the maximum values of average power that the nodes can consume are below a certain threshold (depending on the whole system parameters), no positive solution for R can be found, i.e., the problem does not have a feasible solution.

With reference to the network topology in Figure 2 (left) and under the same settings as above, Figure 5 shows the optimal achieved rate, R^*, versus the maximum transmit power $P_{\rm tx}^{\max}$, in absence of energy constraints. Solid lines refer to the case where the radio range is $d_r = 60$ m, and the network graph is that of Figure 2 (left). Dashed lines instead refer to the case where the network is fully connected ($d_r = 120$ m), i.e., every node can communicate directly with any other node in the network. In both cases, the rate R^* has been computed by using (9) and by considering that nodes can perform either multiuser detection (MUD) or single-user processing (no MUD). We observe that higher data rates can be achieved when MUD is used, at the price of a larger number of states J, and that such benefit holds especially for larger radio ranges. The reason for this behavior is that MUD allows for a better exploitation of links characterized by lower SNR, whose number significantly increases when communications between distant nodes are considered. On the contrary, when nodes can only perform single-user processing, an increase of the radio range provides little gain in the achievable rate, as most of the additional links that are created cannot be efficiently used.

These observations are confirmed by Figure 6, which refers to the same network scenario above, but with $a = 2$. However, with respect to Figure 5, we note that a larger node radio range now leads to a significant improvement in the network rate in both cases, with and without MUD. Indeed, the better signal propagation always allows nodes to efficiently exploit links with far-away nodes, thus to transfer data toward the gateway more swiftly.

VI. CONCLUSIONS

We presented a framework to find communication strategies maximizing the communication rates in wireless networks where nodes may relay each other's traffic, work in half-duplex mode, and may be subject to constraints on their average power consumption. We dealt with the case where nodes can also perform multiuser processing. Our approach leverages linear optimization, and can be applied to any network with arbitrary topology. In addition, the communication strategies that we attain can account for the fact that nodes may have different traffic demands and, consequently, they can provide nodes with a fair rate allocation.

ACKNOWLEDGMENTS

This paper was made possible by NPRP grant $\sharp/5-782-2-322$ from the Qatar National Research Fund (a member of Qatar Foundation). The statements made herein are solely the responsibility of the authors.

REFERENCES

[1] H. Kwon, H. Lee, and J.M. Cioffi, "Cooperative Strategy by Stackelberg Games under Energy Constraint in Multi-hop Relay Networks", *IEEE Globecom,* Hawaii, USA, 2009.

[2] Z. Zhou, S. Zhou, J. Cui, S. Cui, "Energy-Efficient Cooperative Communication Based on Power Control and Selective Single-Relay in Wireless Sensor Networks," *IEEE Transactions on Wireless Communications*, vol. 7, no. 8, pp. 3066–3078, 2008.

[3] R.-S. Liu, K.-W. Fan, Z. Zheng, P. Sinha, "Perpetual and Fair Data Collection for Environmental Energy Harvesting Sensor Networks," *IEEE/ACM Transactions on Networking*, vol. 19, no. 4, pp. 947–960, 2011.

[4] T.M. Cover, J.A. Thomas, *Elements of Information Theory,* John Wiley & Sons, 1991.

[5] I. Maric, R.D. Yates, "Bandwidth and Power Allocation for Cooperative Strategies in Gaussian Relay Networks," *IEEE Transactions on Information Theory,* vol. 56, no. 4, pp. 1880–1889, 2010.

[6] L. Xie, P.R. Kumar, "Multisource, Multidestination, Multirelay Wireless Networks," *IEEE Transactions on Information Theory,* vol. 53, no. 10, pp. 3586–3595, 2007.

[7] C. Edemen, O. Kaya, "Achievable Rates for the Three User Cooperative Multiple Access Channel," *IEEE WCNC,* Las Vegas, NV, 2008.

[8] C.W. Sung, Q. Wang, K.W. Shum. "Capacity Region of the Linear Four-node Half-duplex Wireless Relay," *IEEE Communications Letters,* vol. 13, no. 4, 2009.

[9] Y. Liu, M. Tao, J. Huang, "An Auction Approach to Distributed Power Allocation for Multiuser Cooperative Networks," *IEEE Transactions on Wireless Communications,* vol. 12, no. 1, pp. 237–247, 2013.

[10] C. Jiang, Y. Shi, Y.T. Hou, W. Lou, H.D. Sherali, "Throughput Maximization for Multi-Hop Wireless Networks with Network-Wide Energy Constraint," *IEEE Transactions on Wireless Communications*, vol. 12, no. 3, pp. 1255–1267, 2013.

[11] Z. Hang, T. Dongbao, "City Traffic Detector Optimization Method Study," *Journal of Wuhan University of Technology,* vol. 32, no. 6, pp. 1161–1164, 2008.

[12] A. Nordio, C.F. Chiasserini, A. Tarable "Bounds to Fair Rate Allocation and Communication Strategies in Source/Relay Wireless Networks," *Transactions on Wireless Communications*, vol. 13, no. 1, pp. 320–329, Jan. 2014. 2013.

[13] T. Lutz, C. Hausl, R. Koetter, "Bits Through Deterministic Relay Cascades with Half-Duplex Constraint," *IEEE Transactions on Information Theory*, vol. 58, no. 1, pp. 369–381, 2012.

[14] S. Pollin, B. Bougard, R. Mangharam, F. Catthoor, I. Moerman, R. Rajkumar, L. Van der Perre, "Optimizing Transmission and Shutdown for Energy-efficient Real-time Packet Scheduling in Clustered Ad Hoc Networks," *EURASIP Journal on Wireless Communications and Networking*, vol. 2005, no. 5, Oct. 2005.

[15] K. Rajgopal, S. Wei, "Scheduling with Rate and Duty-Cycle Constraints for Wireless Networks over an Interference Channel," *40th Annual Conference on Information Sciences and Systems,* Princeton, NJ, Mar. 2006.

[16] J.-H. Chang, L. Tassiulas, "Energy Conserving Routing in Wireless Adhoc Networks," *IEEE INFOCOM*, Mar. 2000.

[17] R. Madan, S. Cui, S. Lall, A.J. Goldsmith, "Modelling and Optimization of Transmission Schemes in Energy-constrained Wireless Sensor Networks," *IEEE/ACM Transactions on Networking,* vol. 15, no. 6, pp. 1359–1372, 2007.

[18] P.S. Khairnar, N.B. Mehta, "Insights into Optimal Discrete Rate Adaptation for Average Power Constrained Single and Multi-Node Systems," *IEEE Transactions on Wireless Communications,* vol. 11, no. 2, pp. 537–543, 2012.

[19] M. Noori, M. Ardakani, "On the Achievable Rates of Symmetric Gaussian Multi-way Relay Channels," *EURASIP Journal on Wireless Communications and Networking,* vol. 11, no. 1, 2013.

[20] L. Li, Y. Jing, H. Jafarkhani, "Interference Cancellation at the Relay for Multi-User Wireless Cooperative Networks," *IEEE Transactions on Wireless Communications*, vol. 10, no. 3, pp. 930–939, 2011.

[21] M.R.A. Khandaker, Y. Rong, "Performance Measure of Multi-User Detection Algorithms for MIMO Relay Network," *Postgrad. Electr. Eng. and Comp. Symp. (PEECS)*, Oct. 2009.

[22] A.H. Phan, H.D. Tuan, H.H. Kha, H.H. Nguyen, "Beamforming Optimization in Multi-User Amplify-and-Forward Wireless Relay Networks," *IEEE Transactions on Wireless Communications*, pp. 1510–1520, 2012.

[23] J. Liu, T. Y. Park, Y. T. Hou, Y. Shi, and H. D. Sherali, "Cross-Layer Optimization of MIMO-Based Mesh Networks Under Orthogonal Channels," *IEEE WCNC*, pp. 49–54, Mar. 2007.

[24] A. Nordio, C.F. Chiasserini, A. Tarable "Achievable Rate and Power Consumption in Source/Relay Wireless Networks," *IEEE-APS APWC*, Sept. 2013.

[25] Y. Xie, Y.C. Eldar, A. Goldsmith, "Reduced-Dimension Multiuser Detection," *IEEE Transactions on Information Theory*, vol. 59, no. 6, pp. 3858–3874, 2013.

[26] B. Karp, H.T. Kung, "Greedy Perimeter Stateless Routing for Wireless Networks," *ACM MobiCom*, pp. 243–254 Aug. 2000.

[27] V. Forutan, A. Nordio, C.F. Chiasserini, "Cooperative Communication Strategies for Cascaded Sources/Relays in Wireless Networks," *Global Information Infrastructure and Networking Symposium (GIS)*, Oct. 2013.

[28] S. Verdú, *Multiuser Detection,* Cambridge, U.K.: Cambridge Univ. Press, 1998.

[29] J. Mattingley, S. Boyd, "Real-time Convex Optimization in Signal Processing," *IEEE Signal Processing Magazine*, no. 27, vol. 3, 2010.

[30] Y. Wang, W. Wang, X. Li, W. Song, "Interference-Aware Joint Routing and TDMA Link Scheduling for Static Wireless Networks," *IEEE Transactions on Parallel and Distributed Systems*, vol. 19, no. 12, pp. 1709–1725, 2008.

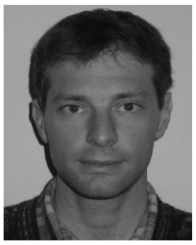

Alessandro Nordio (S'00-M'03) is a researcher at the CNR-IEIIT. In 2002 he received the Ph.D. from "Ecole Polytechnique Federale de Lausanne", Switzerland. From 1999 to 2002, he performed active research with Eurecom Institute, Sophia Antipolis (France). From 2002 to 2009 he was a postdoc researcher with the Electronic Department of Politecnico di Torino, Italy. His research interests are in the field of signal processing, space-time coding, wireless sensor networks and theory of random matrices.

Carla-Fabiana Chiasserini (M'98, SM'09) received her Ph.D. from Politecnico di Torino in 2000. She was a visiting researcher at UCSD in 1998–2003, and she is currently an Associate Professor with the Electronics and Telecommunications Department at Politecnico di Torino. Her research interests include architectures, protocols, and performance analysis of wireless networks. Dr. Chiasserini has published over 200 papers in prestigious journals and leading international conferences, and she serves as Associated Editor of several journals.

Alberto Tarable (S'00-M'02) received the Ph.D. degree in Electronic Engineering in February 2002, both from Politecnico di Torino. From 2002 to 2012, he worked as a researcher in the Department of Electronics and Telecommunications of Politecnico di Torino. From 2012, he holds a research position in the Institute of Electronics, Computer and Telecommunication Engineering of the Italian National Research Council. His research interests include MIMO systems and space-time coding, anytime coding and coding schemes for relay channels.